

PDES WITH COMPRESSED SOLUTIONS

RUSSEL E. CAFLISCH, STANLEY J. OSHER, HAYDEN SCHAEFFER, AND GIANG TRAN

ABSTRACT. Sparsity plays a central role in recent developments in signal processing, linear algebra, statistics, optimization, and other fields. In these developments, sparsity is promoted through the addition of an L^1 norm (or related quantity) as a constraint or penalty in a variational principle. We apply this approach to partial differential equations that come from a variational quantity, either by minimization (to obtain an elliptic PDE) or by gradient flow (to obtain a parabolic PDE). Addition of an L^1 term in the variational method leads to a modified PDE in which there is a subgradient term with a simple explicit form. The resulting parabolic PDEs are L^1 contractive, total variation diminishing, and positivity preserving. Also, the solutions have finite support and finite speed of propagation. Numerical solutions illustrate these analytic results and suggest additional properties of the solutions.

1. INTRODUCTION

Sparsity has played a central role in recent developments in fields such as signal processing, linear algebra, statistics and optimization. Examples include compressed sensing [7, 11], matrix rank minimization [20], phase retrieval [5] and robust principal component analysis [6, 10, 19], as well as many others. A key step in these examples is the use of an L^1 norm (or related quantity) as a constraint or penalty term in a variational formulation. In all of these examples, sparsity is for the coefficients (*i.e.*, only a small set of coefficients are nonzero) in a well-chosen set of modes for representation of the corresponding vectors or functions.

The use of sparse techniques in physical sciences and partial differential equations (PDEs) has been limited, but recent results have included numerical solutions of PDEs with multiscale oscillatory solutions [21], efficient material models derived from quantum mechanics calculations [15], “compressed modes” for variational problems in mathematics and physics [16], and “compressed plane waves” [17]. In the latter two examples, sparsity is used in a new way, in that the solutions are sparse and localized in space (as opposed to sparsity of the coefficients in some modal representation). Some recent extensions of these results have appeared in [2, 23].

Motivated by these examples, we study PDEs that come from a variational principle that includes L^1 terms. The PDE is either an elliptic PDE coming from a

2000 *Mathematics Subject Classification.* 35A99, 65K10.

Key words and phrases. Sparsity, Compressive Sensing, PDE.

The first author was supported in part by DOE grant de-sc0010613.

The second author was supported in part by ONR grants: N000141210838, N000141110749, N000141110719 and by an Army MURI subcontract from Rice University.

The third author was supported by NSF grant DMS-1303892 and the UC President’s Postdoctoral Fellowship program.

The fourth author was supported in part by UC Lab 12-LR-236660.

variational principle or a parabolic PDE coming from a gradient flow of a variational quantity. In either case, the L^1 term in the variational quantity leads to a subgradient term in the PDE. Fortunately, the subgradient term has a simple explicit form, so that the PDEs are amenable to analysis and computation.

The goal of this paper is to derive qualitative properties of these PDEs with subgradient terms - such as well-posedness, finite support, positivity and finite propagation speed - and to present analytic solutions, asymptotic approximations and numerical solutions that illustrate the properties of the PDEs.

To the best of our knowledge there have been no previous treatments of PDEs with subgradient terms. The results described here are intended to provide a theoretical framework for such PDEs and to demonstrate the control on the solution (*e.g.*, on the size of its support) that can be achieved through the inclusion of L^1 subgradient terms. We expect these results to have many applications; *e.g.*, efficient numerical methods for high dimensional problems (*e.g.*, density functional theory [18]), empirical mode decomposition [13], and mathematical modeling, but these applications are beyond the scope of the present work.

Our starting point is a variational quantity

$$(1.1) \quad E(u) = \int \frac{1}{2}(\nabla u) \cdot M(\nabla u) - uf + \mu|u|dx,$$

where $\mu \geq 0$, $M = M(x)$ is a symmetric, positive definite matrix as a function of x , and $f = f(x)$ or $f = f(x, t)$ will be a specified function depending on x or (x, t) . Define the partial differential operator $A[u] = -\nabla \cdot (M\nabla u)$. Minimization of $E(u)$ for $f = f(x)$ leads to the following elliptic PDE

$$(1.2) \quad A[u] = f - \mu p(u),$$

and gradient descent $\partial_t u = -\partial_u E[u]$, starting from initial data $g(x)$, leads to the following parabolic PDE

$$(1.3) \quad \begin{aligned} u_t + A[u] &= f - \mu p(u) \\ u(x, 0) &= g(x), \end{aligned}$$

in which $p(u)$ is a subgradient of $\|u\|_{L^1}$, *i.e.*, $\|v\|_1 \geq \|u\|_1 + \langle v - u, p(u) \rangle$, for any u and v , where $\langle \cdot, \cdot \rangle$ denotes the L^2 inner product.

Our results come from two observations about the PDEs (1.2) and (1.3). First, the subgradient $p(u)$ can be found explicitly in terms of the local values of u and f (see Section 2). Second, the nonlinear PDEs (1.2) and (1.3) can be replaced by linear PDEs with free boundaries, in which the effect of the subdifferential is replaced by a piecewise continuous force (see Section 4).

The paper is divided as follows: in Section 2, we provide the general formulation of the problem and existence theory. In Section 3, we present various properties of solutions to the modified PDEs, such as finite support (*i.e.*, support of finite measure), L^1 contraction, total variation diminishing (TVD), finite speed of propagation, and maximum and comparison principles. Next, some analytic results on the free boundary of the modified PDEs are discussed in Section 4. The numerical implementation and simulations are presented in Sections 5 and 6, and we conclude in Section 7.

2. FORMULATION AND EXISTENCE THEORY

2.1. Formulation. The subgradient can be explicitly identified as

$$(2.1) \quad p(u) = \begin{cases} \text{sign}(u) & \text{if } |u| > 0 \\ \underset{|q| \leq 1}{\text{argmin}} |f - \mu q| & \text{if } u = 0. \end{cases}$$

Note that if $u = 0$ and $|f(x)| \leq \mu$, then $p = f(x)/\mu$. This specification for u was proved in general in [1, 4]. It can be shown directly from Equations (1.2) and (1.3), as follows. For $u = 0$ in an open set, the left side of the equations is 0 so that $f(x) - \mu p(u) = 0$, which is only possible if $f(x) \leq \mu$ and $p(u) = f(x)/\mu$. The value of $p(u)$ on a lower dimensional set does not matter, since the value of the forcing terms on a lower dimensional set does not affect the solution u of the differential equations. For the elliptic equation (1.2) one can also show directly that this identification of $p(u)$ gives $u = 0$ as the unique minimizer of $E(u)$, see Section 3.1 below.

At the interface between a region where $u \neq 0$ and a region where $u = 0$, the natural boundary condition is

$$(2.2) \quad u = 0, \quad \frac{\partial u}{\partial n} = 0.$$

In one dimension the second condition Equation (2.2) simplifies to $u_x = 0$.

At a number of places in the manuscript, we will simplify the presentation by assuming that $x \in \mathbb{R}^1$ and that $M = 1$, so that the elliptic PDE (1.2) becomes Laplace's equation with nonlinear forcing:

$$(2.3) \quad u_{xx} = -f + \mu p(u),$$

and the parabolic PDE (1.3) becomes the heat equation with nonlinear forcing:

$$(2.4) \quad \begin{aligned} u_t - u_{xx} &= f - \mu p(u) \\ u(x, 0) &= g(x). \end{aligned}$$

2.2. Existence Theory. In this section we recall the established existence theory for the elliptic equation (1.2) and the parabolic equation (1.3), based on their variational formulation. In the arguments below, we assume that the domain is bounded, but this should hold more generally.

The elliptic PDE (1.2) comes from minimization of the variational quantity $E(u)$ which is coercive and convex and whose admissible set is the Sobolev space H^1 with norm $\|u\|_{H^1}^2 = \int (|\nabla u|^2 + u^2) dx$. From the calculus of variations, one can show (e.g., Theorems 2 and 3, Section 8.2 of [12]) that there is a unique minimizer u of E on $(H^1, \|\cdot\|_{H^1})$. By using the Poincare inequality, the linear term $\int u f dx$ in $E(u)$ is bounded by $c_1 \int |\nabla u|^2 dx + c_2$ for an arbitrarily small constants c_1 and (possibly large) constant c_2 , so that $E(u)$ is coercive. Uniqueness depends on having a bounded open domain with prescribed boundary data. From calculus of variations, we know that when Equation (1.2) has a unique solution then it agrees with the steady state solution of Equation (1.3).

Next we show for the elliptic PDE, Equation (2.3), that the solution $u \in C^1$. This can be shown by taking the integral over $[x - \epsilon_1, x + \epsilon_2]$ for some $\epsilon_1, \epsilon_2 > 0$:

$$(2.5) \quad \int_{x-\epsilon_1}^{x+\epsilon_2} u_{xx} dx = - \int_{x-\epsilon_1}^{x+\epsilon_2} f dx + \mu \int_{x-\epsilon_1}^{x+\epsilon_2} p(u) dx.$$

and for bounded force, we have the following:

$$(2.6) \quad |u_x(x + \epsilon_2) - u_x(x - \epsilon_1)| \leq (\epsilon_1 + \epsilon_2) (\|f\|_{L^\infty} + \mu).$$

Sending ϵ_1 and ϵ_2 to zero, we see that u_x must be continuous. In higher dimensions, the continuity result above can be deduced directly from the Green's function formulation presented in Section 4.

The following theorem shows that the parabolic PDE (1.3) is well-posed.

Theorem 2.1. *Let $F[u] := A[u] - f + \mu \partial \|u\|_{L^1}$, in which A is defined in Section 1. Then A is maximal monotone and for each $g \in D(F)$ (the domain of F), there exists a unique function $u \in C(L^2; [0, \infty))$ with $u_t \in L^\infty(L^2; (0, \infty))$ such that*

- i) $u(x, 0) = g$ and $u(x, t) \in D(F)$,
- ii) $u_t \in -F[u]$ for a.e. $t \geq 0$,
- iii) Let $u(\cdot)$ and $v(\cdot)$ be the solutions issued from initial data g_1 and g_2 . Then for $t_2 \geq t_1 \geq 0$, $\|u(t_2) - v(t_2)\|_{L^2} \leq \|u(t_1) - v(t_1)\|_{L^2}$.

This theorem follows from the theory of nonlinear semigroups, see for example, Theorem 2 from [9], Theorem 1, Section 3.4 of [1], and Theorem 3, Section 9.6 of [12].

3. VARIOUS PROPERTIES

3.1. Finite Support. The most important result of this work is that the solutions of the elliptic and parabolic problems have support with finite measure, which we show in this section, with particular bounds on the size. In one dimension, using the bounds provided in this section and connectedness arguments, the compactness of the support set can be deduced.

First, observe that if $\mu \geq \max |f|$, then the unique solution of Equation (1.2) is $u \equiv 0$. Indeed, if $u = 0$, since $\frac{f}{\mu} \in [-1, 1]$, we can choose $p(u) = \frac{f}{\mu}$ and Equation (1.2) is satisfied.

Now, take a domain \mathcal{S} on which u is signed and zero on the outside. Integrating both sides of Equation (1.2) gives us

$$(3.1) \quad \int_{\partial \mathcal{S}} M \nabla u \cdot N ds = - \int_{\mathcal{S}} f dx + \mu \text{sign}(u) |\mathcal{S}|.$$

By continuity of the derivatives, along the boundary we must have that the left hand side vanishes. So

$$(3.2) \quad |\mathcal{S}| = \text{sign}(u) \mu^{-1} \int_{\mathcal{S}} f dx.$$

More generally, for any $u \in C^1$, which has a single sign in the domain \mathcal{S} and is zero on the boundary, we have

$$(3.3) \quad |\mathcal{S}| \leq \mu^{-1} \int_{\mathcal{S}} |f| dx.$$

It follows that the support of u satisfies

$$(3.4) \quad |\text{supp}(u)| \leq \mu^{-1} \int_{\text{supp}(u)} |f| dx.$$

A slight modification of (3.4) shows that for any nonnegative α and β with $\alpha + \beta = 1$ that

$$(3.5) \quad |\text{supp}(u)| \leq (\alpha\mu)^{-1} \int (|f| - \beta\mu)^+ dx.$$

In this inequality, the superscript $+$ denotes the positive part; *i.e.*, $(x)^+ = \max(x, 0)$. If f is bounded and $f(x) \rightarrow 0$ as $|x| \rightarrow \infty$, then the set on which $|f(x)| > \beta\mu$ is finite, so that the right hand side of (3.5) is finite, which shows that the support of u has finite measure for the elliptic equation (1.2).

For the parabolic case, the support set will satisfy a differential balancing equation. Again, take a domain $\mathcal{S}(t)$ on which $u > 0$ and vanishes on the boundary. Differentiating the integral of u over $\mathcal{S}(t)$ and using the boundary conditions (*i.e.*, $u = 0$ on $\partial\mathcal{S}(t)$) yields:

$$\begin{aligned} \frac{d}{dt} \int_{\mathcal{S}(t)} u(x, t) dx &= \int_{\mathcal{S}(t)} u_t dx \\ &= \int_{\mathcal{S}(t)} \nabla \cdot M \nabla u + f - \mu p(u) dx. \end{aligned}$$

Because of the divergence theorem and the fact that M is positive definite, we have

$$\frac{d}{dt} \int_{\mathcal{S}(t)} u(x, t) dx \leq \int_{\mathcal{S}(t)} f dx - \mu |\mathcal{S}(t)|.$$

The same argument holds for $u < 0$, which altogether is equivalent to an estimate on the flux:

$$\frac{d}{dt} \int_{\mathcal{S}(t)} |u(x, t)| dx \leq \int_{\mathcal{S}(t)} |f| dx - \mu |\mathcal{S}(t)|.$$

The support set is chosen in order to solve this evolution equation, balancing between the value of f and the parameter μ . Integrating the expression in time yields the following bound on the support size:

$$(3.6) \quad |\text{supp}_{(x,t)} u(x, t)| \leq \int_{\mathcal{S}(t)} |g| dx + \iint_{\mathcal{S}(t)} |f| dx dt.$$

Also, similar to the elliptic case, we have

$$(3.7) \quad |\text{supp}_{(x,t)} u(x, t)| \leq (\alpha\mu)^{-1} \left(\int |g| dx + \iint (|f| - \beta\mu)^+ dx dt \right),$$

for any nonnegative α and β with $\alpha + \beta = 1$. If g is in L^1 and if f is bounded with $f(x) \rightarrow 0$ as $|x| \rightarrow \infty$, this shows that the support of u has finite measure (in (x, t)) for the parabolic equation (1.3).

3.2. L^1 Contraction and Total Variation Diminishing. Let u and v be solutions of Equation (2.4) with initial data $g(x)$ and $h(x)$, respectively. First, note that for any subgradient p of a convex functional, we have

$$(3.8) \quad \text{sign}(u - v)(p(u) - p(v)) \geq 0.$$

We wish to show that the solutions are L^1 contractive and TVD by computing the following:

$$\begin{aligned}
\frac{d}{dt} \|u - v\|_{L^1} &= \frac{d}{dt} \int_{|u-v|>0} |u - v| dx \\
&= \int_{|u-v|>0} \text{sign}(u - v)(u_t - v_t) dx \\
&= \int_{|u-v|>0} \text{sign}(u - v)(u - v)_{xx} - \mu \text{sign}(u - v)(p(u) - p(v)) dx.
\end{aligned}$$

From the arguments in Section 3.1 and from Equation (3.8), we have $\frac{d}{dt} \|u - v\|_{L^1} \leq 0$, and thus the modified PDE is an L^1 contraction. Moreover, if we take $h(x) = g(x + \delta)$ for any $\delta > 0$ we have

$$\frac{d}{dt} \|u(x, t) - u(x + \delta, t)\|_{L^1} \leq 0.$$

Dividing the equation above by δ and taking the supremum over all δ , the following inequality holds:

$$\frac{d}{dt} \|u\|_{TV} \leq 0.$$

Therefore, Equation (2.4) is TVD.

3.3. Entropy Condition. The L^1 contraction and TVD results are directly analogous to those that are obtained by solving the viscosity regularized nonlinear conservation laws:

$$w_t^\epsilon = \epsilon w_{xx}^\epsilon - f(w^\epsilon)_x,$$

for $\epsilon > 0$. Then by letting $\epsilon \rightarrow 0$, one recovers the unique inviscid limit, see [14].

We can also easily obtain an “entropy inequality” in the same spirit. Consider the scaled modified heat equation:

$$(3.9) \quad u_t = \epsilon u_{xx} - \mu p(u).$$

We deliberately put an ϵ in front of the diffusion term to emphasize the similarities to the theory of scalar conservation laws. The following argument holds in more general cases.

Let $K(u)$ be a convex function of u with subgradient $q(u)$. Multiplying Equation (3.9) by the subgradient (as in [14]) yields:

$$(3.10) \quad \frac{d}{dt} K(u) \leq \epsilon \frac{d^2}{dx^2} K(u) - \mu q(u)p(u).$$

For example, if $K(u) = |u|$, then whenever $u \neq 0$, we have

$$(3.11) \quad |u|_t \leq \epsilon |u|_{xx} - \mu.$$

This also gives the strong maximum principle explained in Theorem 3.1 (v).

We integrate Equation (3.10) over the region $\mathcal{S}(t)$, the support set of $u(x, t)$ defined in Section 3.1, to get

$$(3.12) \quad \frac{d}{dt} \int_{\mathcal{S}(t)} K(u) dx \leq -\mu \int_{\mathcal{S}(t)} q(u)p(u) dx,$$

since the spatial gradient is zero along the boundary. By choosing $K(u) = \frac{1}{a}|u|^a$ for $a \geq 1$, Equation (3.12) provides L^a estimates of the solutions. Furthermore, if $K(u) = (u - c)^+$ for $c > 0$, then

$$(3.13) \quad \frac{d}{dt} \int_{\mathcal{S}_c^+(t)} (u - c)^+ dx \leq -\mu |\mathcal{S}_c^+(t)|,$$

where $\mathcal{S}_c^+(t)$ is the set of x for which $u(x) > c$.

3.4. Traveling Wave. To demonstrate finite speed of propagation, consider the 1D-traveling wave solution $u(x, t) = v(s)$ for $s = x - \sigma t$, of the Equation (2.4) with no forcing term. To be specific, we will assume that $v(s) \geq 0$ for $s \geq 0$ and $v(s) = 0$ for $s \leq 0$. We see that v must satisfy the ODE

$$(3.14) \quad v_{ss} + \sigma v_s - \mu = 0,$$

subject to the conditions

$$(3.15) \quad v(0) = v'(0) = 0.$$

The general solution of Equation (3.14) is

$$(3.16) \quad v(s) = \begin{cases} \frac{\mu}{\sigma} s + c_1 e^{-\sigma s} + c_2, & s \geq 0 \\ 0, & \text{otherwise.} \end{cases}$$

The boundary conditions imply

$$c_1 = -c_2 = \frac{\mu}{\sigma^2},$$

so that the traveling wave solution of Equation (2.4) is

$$u(x, t) = \begin{cases} \frac{\mu}{\sigma}(x - \sigma t) + \frac{\mu}{\sigma^2}(e^{-\sigma(x - \sigma t)} - 1), & x \geq \sigma t \\ 0, & \text{otherwise.} \end{cases}$$

We see that in this case we have one sided support.

3.5. An Exact Solution. We construct the exact solution of Equation (2.3) with nonnegative force $f = (1 + x^2)^{-3/2}$ and $\mu \in [0, 1]$. The exact solution is given explicitly by:

$$u = \begin{cases} -(1 + x^2)^{1/2} + \frac{1}{2}\mu x^2 + c, & |x| \leq a \\ 0, & |x| > a. \end{cases}$$

where,

$$c = \frac{\mu + \mu^{-1}}{2}, \quad a = \sqrt{\mu^{-2} - 1}.$$

The boundary value a and constant c are determined so that $u(\pm a) = u_x(\pm a) = 0$. At the boundary of the support, $f(\pm a) = \mu^3 < \mu$. The results show that the solution is nonnegative for nonnegative f , and that having $|f(x)| \leq \mu$ does not imply $p(u(x)) = \frac{f(x)}{\mu}$.

3.6. Maximum and Comparison Principles. The modified PDE still retains some of the properties of the original PDE. Here we derive maximum and comparison principles for the elliptic and parabolic equations.

Theorem 3.1. *Let f and g be smooth functions on $x \in \mathbb{R}$. Assume that $f(x) \geq 0$, $g(x) \geq 0$, and that $f(x) \rightarrow 0$ and $g(x) \rightarrow 0$ as $|x| \rightarrow \infty$. Let $v^\mu(x, t)$ satisfy Equation (2.4), $u^\mu(x)$ satisfy Equation (2.3), and assume that $v^\mu(x, t) \rightarrow 0$ and $u^\mu(x) \rightarrow 0$ as $|x| \rightarrow \infty$ for all $t \geq 0$. Then for all x and all $t \geq 0$,*

- (i) $v^\mu(x, t) \geq 0$.
- (ii) $u^\mu(x) \geq 0$.
- (iii) $v^0(x, t) \geq v^\mu(x, t)$.
- (iv) $u^0(x) \geq u^\mu(x)$.
- (v) If $f = 0$, then $\min(g(x) + t\mu, 0) \leq v^\mu(x, t) \leq \max(g(x) - t\mu, 0)$.

Proof. 1. Let ε be any positive number and let (x_1, t_1) be the position and the time when v first attains the value $-\varepsilon$. From the limiting conditions on v^μ , the point x_1 is finite. Then $v_t^\mu(x_1, t_1) \leq 0$ and $v_{xx}^\mu(x_1, t_1) \geq 0$. Also $p(v^\mu) = -1$. Therefore at (x_1, t_1) , the left hand side of Equation (2.4) is nonpositive while the right hand side is strictly positive, which is a contradiction. It follows that $v^\mu(x, t) \geq 0$ for all (x, t) .

2. The same logic shows that $u^\mu(x) \geq 0$ for all x .

3. Define $z = v^0 - v^\mu$. Then $z_t - z_{xx} = \mu p(v^\mu)$ and $z = 0$ for $t = 0$. By (i), we know that $v^0 \geq 0$, $v^\mu \geq 0$, and $p(v^\mu) \geq 0$. Then $z < 0$ implies that $v^\mu > 0$ and $p(v^\mu) = 1$. Since $z = 0$ at $t = 0$ and $z \rightarrow 0$ as $|x| \rightarrow \infty$, then the proof of (i) shows that z cannot be negative at any point.

4. The same logic shows that $u^0(x) \geq u^\mu(x)$, for all x .

5. This follows directly from Equation (3.11). \square

4. A FREE BOUNDARY FORMULATION

In this section, we first present a free boundary formulation of both the elliptic and parabolic PDEs (1.2) and (1.3). Then we analyze the short time behavior of the free boundary - *i.e.* of the support of u - for the parabolic PDE (2.4) in 1D.

4.1. Free Boundary. Assume that $u > 0$, $u < 0$ and $u = 0$ in the sets Ω_+ , Ω_- , and Ω_0 , respectively. Then the solution of the Laplace's equation (2.3) can be written as

$$(4.1) \quad u(x) = \int_{\Omega_+} G(x-y)(f(y) - \mu)dy + \int_{\Omega_-} G(x-y)(f(y) + \mu)dy,$$

and the solution of the heat equation (2.4) can be written as

$$(4.2) \quad \begin{aligned} u(x, t) = & \int G(x-y, t)g(y)dy + \int_0^t \int_{\Omega_+(s)} G(x-y, t-s)(f(y) - \mu)dyds \\ & + \int_0^t \int_{\Omega_-(s)} G(x-y, t-s)(f(y) + \mu)dyds, \end{aligned}$$

in which the Green's function $G(x, t)$ for the heat equation and the Green's function $G(x)$ for the Laplace's equation are given by

$$(4.3) \quad \begin{aligned} G(x) &= |x|/2, \\ G(x, t) &= (4\pi t)^{-1/2} \exp(-x^2/4t). \end{aligned}$$

From these formulas, if f is continuous, then one can see that u is $C^2(x)$ and $C^1(t)$ away from $u = 0$ and that u is $C^1(x)$ everywhere. This is stronger than the regularity provided by Theorem 2.1.

4.2. Boundary Conditions for the Modified Heat Equation. We derive here the natural boundary conditions to Equation (2.4) for a set of forces f and initial data g .

First we show that the two free boundary conditions (2.2) can be replaced by a single boundary condition for the heat flux at a moving interface. The following general lemma shows that the natural boundary condition is on the flux at the free boundary.

Flux Condition. *Let $u(x, t) \in C^0(C^1(\mathbb{R}); (0, T))$ and $u_t \in L^\infty(C^1(\mathbb{R}); (0, T))$ be a solution to*

$$(4.4) \quad u_t - u_{xx} = h(x, t, \mu).$$

Assume that there exists a positive valued function $a \in C^1(0, T)$ such that $h = 0$ for $|x| > a(t)$, $g = 0$ for $|x| > a(0)$, and the exterior mass,

$$m(t) = \int_{a(t)}^{\infty} u(x, t) dx,$$

is conserved, then $u(a(t), t) = 0$ and $u_x(a(t), t) = 0$.

To derive this condition, consider the heat equation (4.4). Differentiate the one sided mass in time yields:

$$\begin{aligned} \frac{dm}{dt} &= -u(a(t), t)a'(t) + \int_{a(t)}^{\infty} u_t(x, t) dx \\ &= -u(a(t), t)a'(t) + \int_{a(t)}^{\infty} u_{xx}(x, t) dx \\ &= -u(a(t), t)a'(t) - u_x(a(t), t) \\ &= -F(t), \end{aligned}$$

in which F is the flux across the moving boundary $x = a(t)$.

We now can see that if the flux across a moving boundary $x = a(t)$ is zero (*i.e.* the mass is conserved), we have

$$(4.5) \quad F(t) = u(a(t), t)a'(t) + u_x(a(t), t) = 0.$$

This is the natural boundary condition for this problem.

In the time-dependent region $\mathcal{F} = \{(x, t) : x > a(t)\}$, the initial data g , force h and incoming flux F are all zero, so that the solution is identically zero. In particular, $u = u_x = 0$ on $x = \pm a(t)$.

4.3. Finite Speed of Propagation from the Continuous Formulation. Consider the following equation

$$(4.6) \quad u_t - u_{xx} = \begin{cases} f(x) - \mu, & |x| < a(t) \\ 0, & |x| > a(t) \end{cases}$$

$$(4.7) \quad u(x, 0) = g(x).$$

For simplicity assume that $f(x) = f(|x|)$ and $g(x) = g(|x|)$, and that $f(|x|)$ and $g(|x|)$ are decreasing functions with $f(|x|) \rightarrow 0$ and $g(|x|) \rightarrow 0$ as $|x| \rightarrow \infty$.

4.3.1. $f \neq 0$ and $g = 0$.

Denote $a_0 \geq 0$ such that $f(a_0) = \mu$ and assume that $f_x(a_0) \neq 0$. By studying the exterior mass of Equation (4.6), we want to show that in small time, we can have an approximation of the boundary

$$(4.8) \quad a(t) = a_0 + a_1 \sqrt{t},$$

for some $a_1 \geq 0$. With this in mind, we can derive an approximation form of the free boundary in short time.

We look for an increasing function $a(t)$ such that the exterior mass of Equation (4.6) is zero:

$$(4.9) \quad m(t) = \int_{a(t)}^{\infty} dx \int_0^t ds \int_{-a(s)}^{a(s)} G(x-y, t-s)(f(y) - \mu) dy.$$

We first want to simplify Equation (4.9) for small t . Since $a(t)$ is an increasing function, we have

$$y \leq a(s) \leq a(t) \leq x.$$

Therefore, for t small, the Green's function $G(x-y, t-s)$ is sharply peaked near the point

$$y = a(t), \quad s = t, \quad x = a(t).$$

So we can replace $(f(y) - \mu)$ by the first few terms in its Taylor expansion

$$(4.10) \quad f(y) - \mu = (y - a_0)f_1 + \mathcal{O}((y - a_0)^2),$$

in which $f_1 = f_x(a_0)$. Also, since $G(x-y, t-s)$ decays exponentially as $y \rightarrow -\infty$, we replace the lower limit $y = -a(s)$ by $-\infty$. Now the mass can be approximated by

$$(4.11) \quad m(t) = f_1 \int_{a(t)}^{\infty} dx \int_0^t ds \int_{-\infty}^{a(s)} (y - a_0) G(x-y, t-s) dy$$

Next we show the existence of a_1 satisfying the following approximations

$$(4.12) \quad a(t) = a_0 + a_1 \sqrt{t}, \quad \text{and} \quad m(t) = 0.$$

We change the variables to

$$(4.13) \quad \begin{aligned} x &= x_1 \sqrt{t} + a_0, & x_1 &\in [a_1, \infty), \\ y &= y_1 \sqrt{t} + a_0, & y_1 &\in (-\infty, a_1 \sqrt{s_1}], \\ s &= s_1 t, & s_1 &\in [0, 1], \end{aligned}$$

and

$$(4.14) \quad \begin{aligned} x_1 &= x_2 a_1, & x_2 &\in [1, \infty), \\ y_1 &= y_2 a_1, & y_2 &\in (-\infty, \sqrt{s_1}], \end{aligned}$$

and note that $G(x-y, t-s) = t^{-1/2}G(x_1-y_1, 1-s_1) = t^{-1/2}G(a_1(x_2-y_2), 1-s_1)$. Then

$$\begin{aligned}
 m(t) &= f_1 t^2 \int_{a_1}^{\infty} dx_1 \int_0^1 ds_1 \int_{-\infty}^{a_1 \sqrt{s_1}} y_1 G(x_1 - y_1, 1 - s_1) dy_1 \\
 &= a_1^3 f_1 t^2 \int_1^{\infty} dx_2 \int_0^1 ds_1 \int_{-\infty}^{\sqrt{s_1}} y_2 G(a_1(x_2 - y_2), 1 - s_1) dy_2.
 \end{aligned}
 \tag{4.15}$$

Consider the rescaled masses $\widetilde{m}_1(a_1) = m(t)/(f_1 t^2)$ and $\widetilde{m}_2(a_1) = m(t)/(a_1^2 f_1 t^2)$; i.e.,

$$\begin{aligned}
 \widetilde{m}_1(a_1) &= \int_{a_1}^{\infty} dx_1 \int_0^1 ds_1 \int_{-\infty}^{a_1 \sqrt{s_1}} y_1 G(x_1 - y_1, 1 - s_1) dy_1, \\
 \widetilde{m}_2(a_1) &= a_1 \int_1^{\infty} dx_2 \int_0^1 ds_1 \int_{-\infty}^{\sqrt{s_1}} y_2 G(a_1(x_2 - y_2), 1 - s_1) dy_2.
 \end{aligned}
 \tag{4.16}$$

As $a_1 \rightarrow 0$, $\widetilde{m}_1(a_1)$ goes to

$$\widetilde{m}_1(0) = \int_0^{\infty} dx_1 \int_0^1 ds_1 \int_{-\infty}^0 y_1 G(x_1 - y_1, 1 - s_1) dy_1
 \tag{4.17}$$

with $\widetilde{m}_1(0) < 0$. This shows that $m(t) < 0$ for $a_1 = 0$.

On the other hand, for $a_1 \gg 1$, $a_1 G(a_1(x_2 - y_2), 1 - s_1)$ is approximately the Dirac delta function at $x_2 = y_2$, $s_1 = 1$. At this point, we have $y_2 > 0$, therefore $\widetilde{m}_2(a_1) > 0$. This shows that $m(t) > 0$ for large values of a_1 . Thus there exists a positive value a_1 so that $m(t) = 0$.

4.3.2. $f = 0$ and $g \neq 0$ with finite support.

We can show similar results for the case of general initial data $g(x)$ provided that $g(x) = 0$ for $|x| \geq a_0$. We look for an increasing function $a(t)$ such that the exterior mass is zero:

$$m(t) = \int_{a(t)}^{\infty} dx \int_{-\infty}^{\infty} G(x-y, t) g(y) dy - \mu \int_{a(t)}^{\infty} dx \int_0^t ds \int_{-a(s)}^{a(s)} G(x-y, t-s) dy.
 \tag{4.18}$$

Again, we take $a(t)$ of the form in Equation (4.8), where a_0 is determined by $g(a_0) = 0$ and $g_x(a_0) \neq 0$.

Since $G(x-y, t-s)$ decays exponentially as $y \rightarrow -\infty$, we replace the lower limit $y = -a(s)$ by $-\infty$ and the mass becomes

$$m(t) = \int_{a(t)}^{\infty} dx \int_{-\infty}^{\infty} G(x-y, t) g(y) dy - \mu \int_{a(t)}^{\infty} dx \int_0^t ds \int_{-\infty}^{a(s)} G(x-y, t-s) dy.
 \tag{4.19}$$

We wish to show the existence of a_1 satisfying the following approximations

$$a(t) = a_0 + a_1 \sqrt{t}, \quad \text{and} \quad m(t) = 0.
 \tag{4.20}$$

Applying the same change of variables Equations (4.13) as the previous section, we have:

$$\begin{aligned} m(t) = & \sqrt{t} a_1^2 \int_1^\infty dx_2 \int_{-\infty}^\infty G(a_1(x_2 - y_2), 1) g(y_2 a_1 \sqrt{t} + a_0) dy_2 \\ & - \mu t^{3/2} a_1^2 \int_1^\infty dx_2 \int_0^1 ds_1 \int_{-\infty}^{\sqrt{s_1}} G(a_1(x_2 - y_2), 1 - s_1) dy_2. \end{aligned}$$

Consider a fixed time $0 < t \ll 1$ and define the function $M(a_1)$ as the mass above. The problem becomes showing the existence of a root of M .

First, for $a_1 \gg 1$, $a_1 G(a_1(x_2 - y_2), 1)$ and $a_1 G(a_1(x_2 - y_2), 1 - s_1)$ are approximately the Dirac delta functions at $(x_2 = y_2)$ and $(x_2 = y_2, s_1 = 1)$, respectively. Notice that $y_2 \in (-\infty, \sqrt{s_1}]$ in the second function. Therefore, the mass can be approximated as

$$(4.21) \quad M(a_1) = \int_{a(t)}^\infty g(x) dx - c \mu t^{3/2} a_1 < 0,$$

since the first term in Equation (4.21) is relatively small due to the integrability condition on g and the second term is relatively large for $a_1 \gg 1$.

Second, for $0 < a_1 \ll 1$ and $s_1 \leq 1$, we have

$$(4.22) \quad \int_1^\infty dx_2 \int_0^1 ds_1 \int_{-\infty}^{\sqrt{s_1}} G(a_1(x_2 - y_2), 1 - s_1) dy_2 \leq \frac{2}{3\sqrt{\pi} a_1^2}.$$

Next, Taylor expanding $g(y_2 a_1 \sqrt{t} + a_0)$ around a_0 to get

$$\begin{aligned} M(a_1) & \geq \int_{a_0 + a_1 \sqrt{t}}^\infty dx \int_{-a_0}^{a_0} G(x - y, t) g(y) dy - \frac{2\mu t^{3/2}}{3\sqrt{\pi}} \\ & = g_x(a_0) \int_{a_0 + a_1 \sqrt{t}}^\infty dx \int_{-\infty}^{a_0} G(x - y, t) (y - a_0) dy - \frac{2\mu t^{3/2}}{3\sqrt{\pi}}. \end{aligned}$$

We change the variables to (x_1, y_1) , which yields

$$M(a_1) \geq g_x(a_0) t \int_{a_1}^\infty dx_1 \int_{-\infty}^0 G(x_1 - y_1, 1) y_1 dy_1 - \frac{2\mu t^{3/2}}{3\sqrt{\pi}} > 0,$$

for small t . Thus there exists a positive value a_1 so that $M(a_1) = 0$ and thereby $m(t) = 0$.

4.3.3. $f = 0$ and $g \neq 0$ with infinite support.

If g is not compactly supported, then this argument can be extended by taking a short time forward. For $0 < t \ll 1$ and $x \gg 1$, by the decay assumption we have $g_{xx} \ll \mu$ (thus $u_{xx} \ll \mu$ in short time) so the PDE is $u_t = -\mu$. This implies that $u(x, t) = g(x) - \mu t$ for large x and small t .

5. NUMERICAL IMPLEMENTATION

Here we present two numerical methods for implementing these PDEs in practice. The first scheme is implicit in which both the subgradient and the diffusion terms must be inverted simultaneously. The second scheme is semi-implicit (also known as explicit-implicit or forward-backward), where the subgradient term is discretized forward in time and the diffusion term is frozen in the current step. Both have their advantages and can be chosen for particular applications.

In this section, we denote h and τ the space and time steps of the finite difference schemes.

5.1. Implicit Equation. Recall the heat equation

$$(5.1) \quad u_t - u_{xx} = f(x) - \mu p(u), \quad u(x, 0) = g(x),$$

which we can discretize implicitly in time, with step size τ , by

$$(5.2) \quad u^{n+1} - u^n - \tau u_{xx}^{n+1} = \tau (f - \mu p(u^{n+1})),$$

where u_{xx}^{n+1} denotes the standard $2d + 1$ point approximation to the Laplacian in d dimensions. The convergence of this scheme is guaranteed, for example see Crandall-Liggett theorem [9]. In general it may be difficult to invert both the second derivative and the subgradient directly. However the solution of Equation (5.2) is the unique minimizer of the following strictly convex functional:

$$(5.3) \quad u^{n+1} = \operatorname{argmin}_v \frac{1}{2} \int \left((v - u^n - \tau f)^2 + \tau (v_x)^2 \right) dx + \mu \tau \int |v| dx.$$

To solve this minimization problem, we use proximal gradient descent to ensure convergence to the correct function. We outline this procedure here.

Taking the first variation of Equation (5.3) and embedding it in a gradient descent evolution yields:

$$(5.4) \quad v_s = -v + u^n + \tau f + \tau v_{xx} - \tau \mu p(v).$$

In this form, v_s is the artificial time derivative of v . Notice that the right hand side of Equation (5.4), whose variational model guarantees the unique minimizer, is the negative of Equation (5.2). Discretizing Equation (5.4) gives us

$$(5.5) \quad \frac{v^{k+1} - v^k}{\sigma} = -v^{k+1} + u^n + \tau f + \tau v_{xx}^k - \tau \mu p(v^{k+1}),$$

where $\sigma > 0$. The solution is:

$$(5.6) \quad v^{k+1} = S \left(\frac{v^k + \sigma (u^n + \tau f + \tau v_{xx}^k)}{1 + \sigma}, \frac{\tau \mu \sigma}{1 + \sigma} \right),$$

in which the shrinkage operator S is the soft-thresholding function defined pointwise as $S(z, \beta) = \max(|z| - \beta, 0) \frac{z}{|z|}$. It is the solution to the problem:

$$S(z, \beta) = \operatorname{argmin}_w \left\{ \beta \|w\|_{L^1} + \frac{1}{2} \|w - z\|_{L^2}^2 \right\}.$$

The sequence $\{v^k\}_k$ generated by Equation (5.6) converges to the unique minimizer v^* , provided $\sigma \leq \frac{h^2}{4\tau}$, see for example [3].

The solution of Equation (5.3) is then $u^{n+1} = v^*$. The procedure transforms Equation (5.2) to an easy to solve fixed point iteration with a guaranteed convergence rate. There is a trade off for the implicit method: the larger we take the timestep τ , the longer it will take to update each timestep.

5.2. Implicit-Explicit Scheme. From the numerical perspective, the multivalued term $p(u)$ is the main source of difficulties. However, since $u + p(u)$ is easy to invert, we may write the discretization as follows:

$$(5.7) \quad u^{n+1} - u^n - \tau u_{xx}^n = \tau(f - \mu p(u^{n+1})),$$

where the diffusion is frozen in time and the subgradient term is discretized in the forward time step. Simplifying Equation (5.7) and inverting the subgradient term leads to:

$$(5.8) \quad u^{n+1} = S(u^n + \tau(u_{xx}^n + f), \tau\mu)$$

with the standard time step restriction: $\tau \leq \frac{h^2}{4}$. This scheme has the advantage of being easy to implement for a general evolution equation.

Remark 5.1. Given any general parabolic evolution $u_t = -A[u]$, let $A_h[u]$ be a monotone and convergent discretization of $A[u]$ on a grid with step size h . Then the implicit-explicit scheme for the modified evolution equation can be written as:

$$(5.9) \quad u^{n+1} = S(u^n - \tau A_h[u^n], \tau\mu),$$

with the same time step restriction as the original scheme. This shows that our proposed methodology is easy to incorporate for any PDE.

6. COMPUTATIONAL SIMULATIONS

In this section we show convergence of our numerical scheme to known solutions, approximations to the support set evolution, and numerical solutions for higher dimension.

6.1. Numerical Convergence. In Figure 1, we solve Equation (2.4) (with $\mu = 0.05$) using the implicit-explicit scheme (Equation (5.8)). The initial data is taken to be the traveling wave profile (Equation (3.16)) with speed $\sigma = 2$. The numerical solution has the correct support set and speed of propagation, validating the traveling wave solution as well as the numerical method. This is further confirmed in Figure 2, where the numerical solution is compared to the exact solution. To compute the error, we use the following norms:

$$\text{Error}_q(h) = \max_n \|u_h^n - u_{exact}\|_q,$$

where $q = 1, 2, \infty$ and u_h^n is the solution at t_n with space resolution h . The errors in these three norms are plotted along side the line representing the second order (dashed line) convergence.

To test the stability of these traveling wave solutions, we initialize our numerical scheme with the traveling wave profile perturbed by uniformly random noise sampled from $[0, 0.05]$. The time evolution is shown in Figure 3. In a short time, the Laplacian term dominates the evolution, which is expected. The solution gradually smooths down to a new traveling wave profile and begins to translate at the expected speed. This shows that the traveling wave solution is an attracting solution, at least locally.

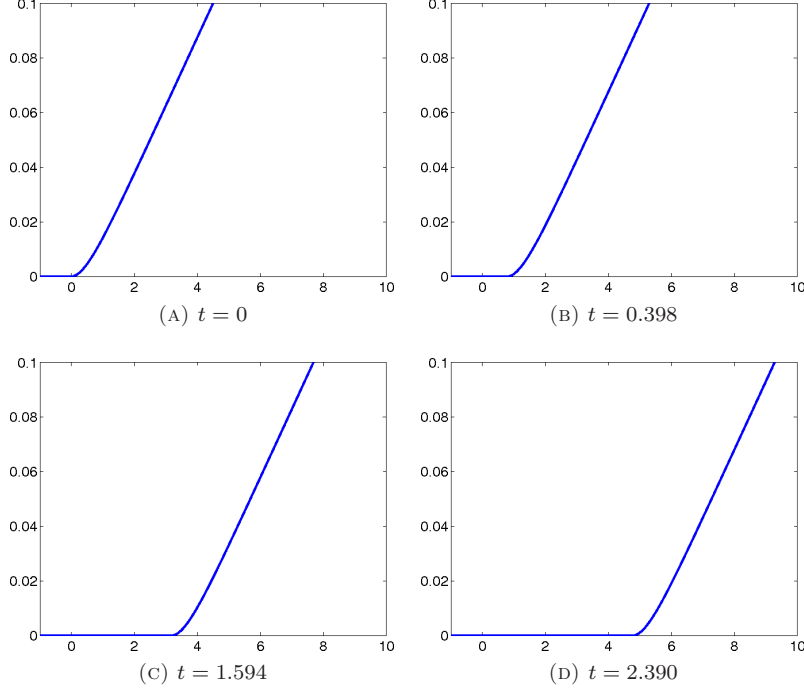


FIGURE 1. Numerical solution starting with an initial traveling wave profile with $\sigma = 2$ and $\mu = 0.05$ computed using 500 grid points.

6.2. One Dimensional Heat Equation. In Figure 4 the plot shows the modified heat equation (Equation (2.4)) with zero initial data and force $f(x) = 2e^{-5x^2}$. The solutions evolves upward in time with their support sets marked by red circles. The corresponding table provides a least squares fit to estimate the coefficient a_1 from Equation (4.8) under grid refinement. We see that the coefficient a_1 approaches the value 1 quickly within some small approximation error.

6.3. Two Dimensional Heat Equation. In Figure 5 we compute the solution of Equation (2.4) with $\mu = 2$ and $f = 0$. The initial data is a smoothed indicator function on the star shaped domain. In Figure 6 the corresponding support set of Figure 5 is shown. The support set grows outward to a maximum size and retracts inward as the solution decays to zero.

6.4. Graph Diffusion. In higher dimensions, we can consider the standard normalized diffusion equation:

$$(6.1) \quad \begin{aligned} u_t &= L_g u := - \left(I - D^{-1/2} \mathcal{A} D^{-1/2} \right) u \\ u(x, 0) &= g(x), \end{aligned}$$

where L_g is the graph Laplacian, \mathcal{A} is the adjacency matrix, and D is the degree matrix. For more on the graph Laplacian, see [8, 22].

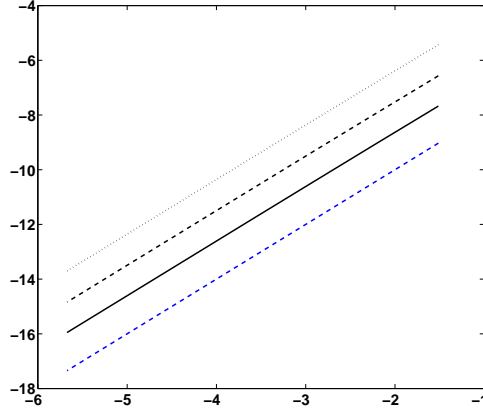


FIGURE 2. Convergence analysis using the L^1 (dotted line), L^2 (dashed line), and L^∞ (solid line) norms in space and L^∞ norm in time. The x -axis is the \log of the grid resolution h and the y -axis is the \log of the Error. The blue dashed lines represents second order convergence.

In Figure 7, the points represent the projection of vectors from \mathbb{R}^{100} and each point is connected to many others in a non-local fashion. For the initial data, we concentrate the mass on one point in the far left, specifically, the $u(x_j, 0) = \delta_{j,1000}$ where $\delta_{j,k}$ is the Kronecker delta function. As the system evolves governed by Equation (6.1), the solution becomes strictly positive quickly.

The modified equation is:

$$(6.2) \quad \begin{aligned} u_t &= - \left(\mathbf{I} - D^{-1/2} \mathcal{A} D^{-1/2} \right) u - \mu p(u) \\ u(x, 0) &= g(x). \end{aligned}$$

In Figure 8 we begin with the same initial condition and see that over time the support set does not grow past a bounded region if u evolves as in (6.2). Therefore, numerically we show that the support is of finite size for the case of graph diffusion. In Figure 8(d) the solution begins to decay to zero which causes its support set to retract towards the initial support before vanishing.

7. CONCLUSION

We have introduced the notion of PDEs with compressed solutions, obtained by adding an L^1 term to standard calculus of variations yielding elliptic and parabolic PDEs with subgradient terms. We show various properties such as finite support, L^1 contraction, TVD, finite speed of propagation, maximum and comparison principles, and short time behavior of the support set. This is all in the spirit of borrowing the key idea from compressed sensing, that L^1 regularization implies sparsity of discrete systems [11], and transferring it to classical problems in PDE. See [16, 17, 21] for earlier work in this direction. We believe many extensions and applications are likely to follow.

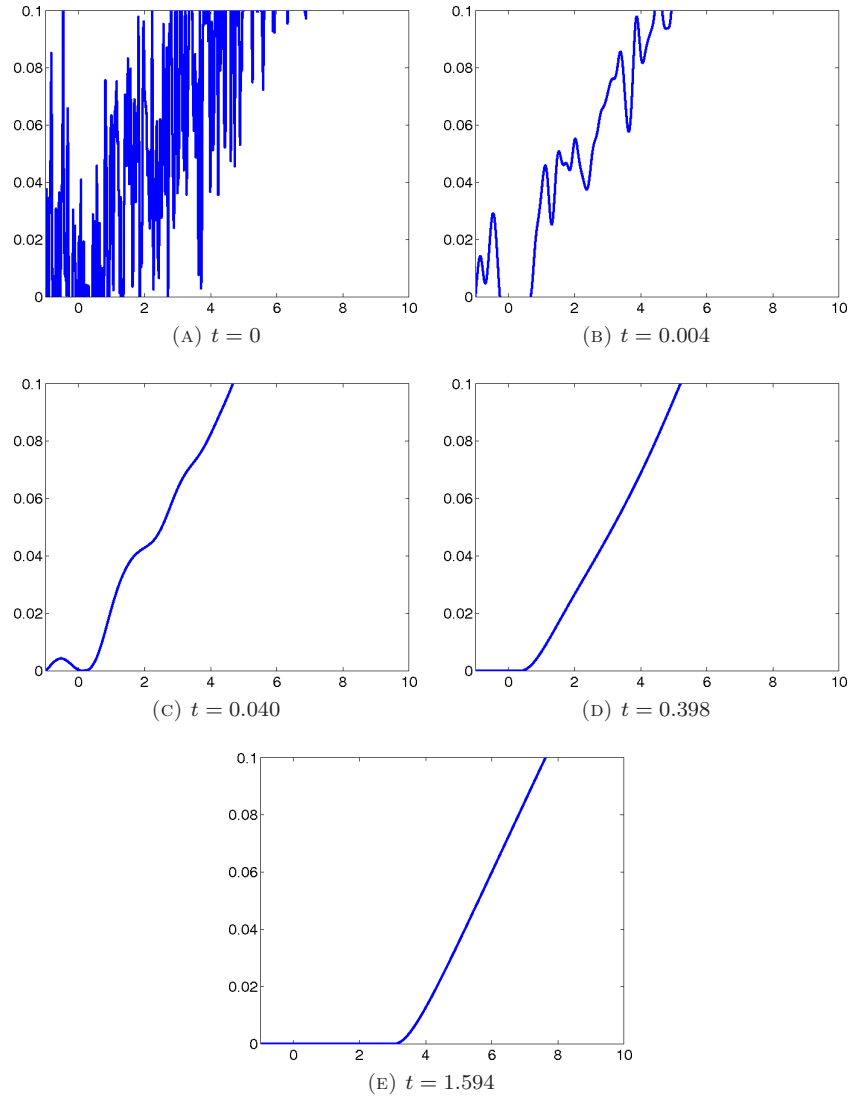


FIGURE 3. Numerical solution starting with an initial traveling wave profile perturbed by uniformly random noise sampled from $[0, 0.05]$ with $\sigma = 2$ and $\mu = 0.05$. This is solved on a grid of 500 points.

ACKNOWLEDGMENTS

The authors would like to thank Farzin Barekat, Jerome Darbon, William Feldman, Inwon C. Kim and James H. von Brecht for their helpful discussions and comments.

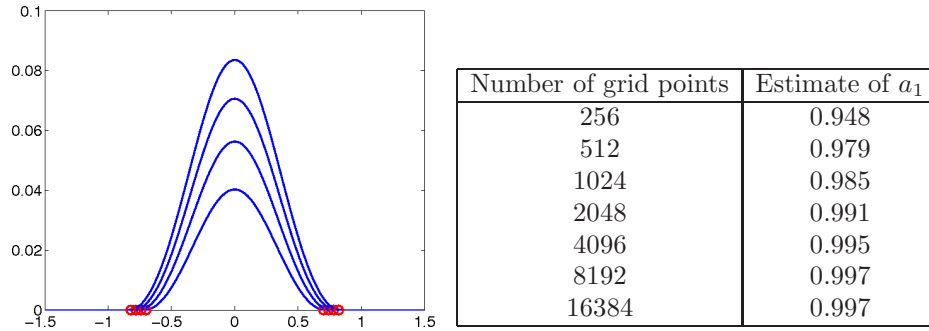


FIGURE 4. The graph is a 1d simulation of the heat equation with the subgradient term, zero initial data, and a Gaussian forcing function centered around zero, $f(x) = 2e^{-5x^2}$. The solutions are growing upward in time and their support set is marked by red circles. The table shows the estimate of the coefficient a_1 from Equation (4.8) under grid refinement.

REFERENCES

- [1] J. P. Aubin and A. Cellina. *Differential inclusions: Set-valued maps and viability theory*. Springer-Verlag New York, Inc., 1984.
- [2] F. Barekat. On the consistency of compressed modes for variational problems. *arXiv preprint arXiv:1310.4552*, 2013.
- [3] A. Beck and M. Teboulle. A fast iterative shrinkage-thresholding algorithm for linear inverse problems. *SIAM Journal on Imaging Sciences*, 2(1):183–202, 2009.
- [4] H. Brezis. *Opérateurs maximaux monotones et semi-groupes de contractions dans les espaces de Hilbert*, volume 5. Access Online via Elsevier, 1973.
- [5] E. J. Candès, Y. C. Eldar, T. Strohmer, and V. Voroninski. Phase retrieval via matrix completion. *SIAM Journal on Imaging Sciences*, 6(1):199–225, 2013.
- [6] E. J. Candès, X. Li, Y. Ma, and J. Wright. Robust principal component analysis? *Journal of the ACM (JACM)*, 58(3):11, 2011.
- [7] E. J. Candès, J. Romberg, and T. Tao. Robust uncertainty principles: Exact signal reconstruction from highly incomplete frequency information. *Information Theory, IEEE Transactions on*, 52(2):489–509, 2006.
- [8] F. R. Chung. *Spectral graph theory*, volume 92. AMS, 1997.
- [9] M. G. Crandall and T. M. Liggett. Generation of semi-groups of nonlinear transformations on general Banach spaces. *American Journal of Mathematics*, 93(2):265–298, 1971.
- [10] A. d’Aspremont, L. El Ghaoui, M. I. Jordan, and G. R. Lanckriet. A direct formulation for sparse PCA using semidefinite programming. *SIAM review*, 49(3):434–448, 2007.
- [11] D. L. Donoho. Compressed sensing. *Information Theory, IEEE Transactions on*, 52(4):1289–1306, 2006.
- [12] L. C. Evans. *Partial differential equations*. Graduate studies in mathematics. *American mathematical society*, 2, 1998.
- [13] N. E. Huang, Z. Shen, S. R. Long, M. C. Wu, H. H. Shih, Q. Zheng, N.-C. Yen, C. C. Tung, and H. H. Liu. The empirical mode decomposition and the Hilbert spectrum for nonlinear and non-stationary time series analysis. *Proceedings of the Royal Society of London. Series A: Mathematical, Physical and Engineering Sciences*, 454(1971):903–995, 1998.
- [14] P. D. Lax. *Hyperbolic systems of conservation laws and the mathematical theory of shock waves*, volume 11. SIAM, 1973.
- [15] L. J. Nelson, G. L. Hart, F. Zhou, and V. Ozoliņš. Compressive sensing as a paradigm for building physics models. *Physical Review B*, 87(3):035125, 2013.
- [16] V. Ozoliņš, R. Lai, R. E. Caflisch, and S. Osher. Compressed modes for variational problems in mathematics and physics. *Proc. NAS*, 2013. To appear.

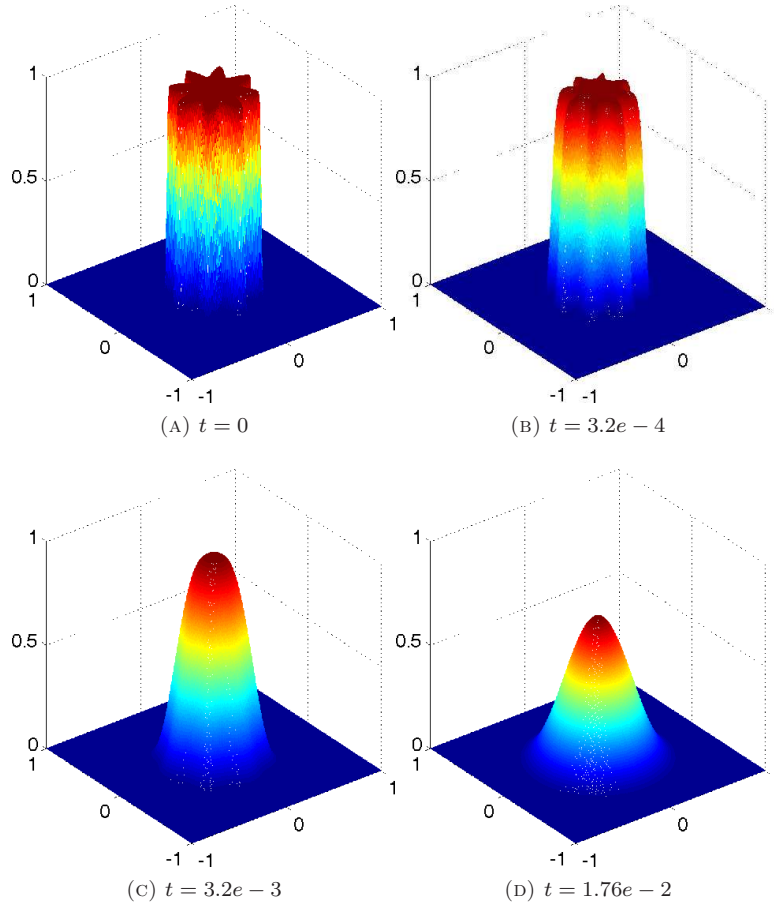


FIGURE 5. Solutions of the initial value problem (no forcing term) computed on a 500 by 500 grid with $\mu = 2$.

- [17] V. Ozoliņš, R. Lai, R. E. Caflisch, and S. Osher. Compressed plane waves - compactly supported multiresolution basis for the laplace operator, 2013. In preparation.
- [18] R. G. Parr and W. Yang. *Density-functional theory of atoms and molecules*, volume 16. Oxford University Press, 1989.
- [19] X. Qi, R. Luo, and H. Zhao. Sparse principal component analysis by choice of norm. *Journal of multivariate analysis*, 2012.
- [20] B. Recht, M. Fazel, and P. A. Parrilo. Guaranteed minimum-rank solutions of linear matrix equations via nuclear norm minimization. *SIAM review*, 52(3):471–501, 2010.
- [21] H. Schaeffer, R. E. Caflisch, C. D. Hauck, and S. Osher. Sparse dynamics for partial differential equations. *Proceedings of the National Academy of Sciences*, 110(17):6634–6639, 2013.
- [22] U. Von Luxburg. A tutorial on spectral clustering. *Statistics and computing*, 17(4):395–416, 2007.
- [23] K. Yin and S. Osher. On the completeness of the compressed modes in the eigenspace. *UCLA Cam Reports: 13-62*, 2013.

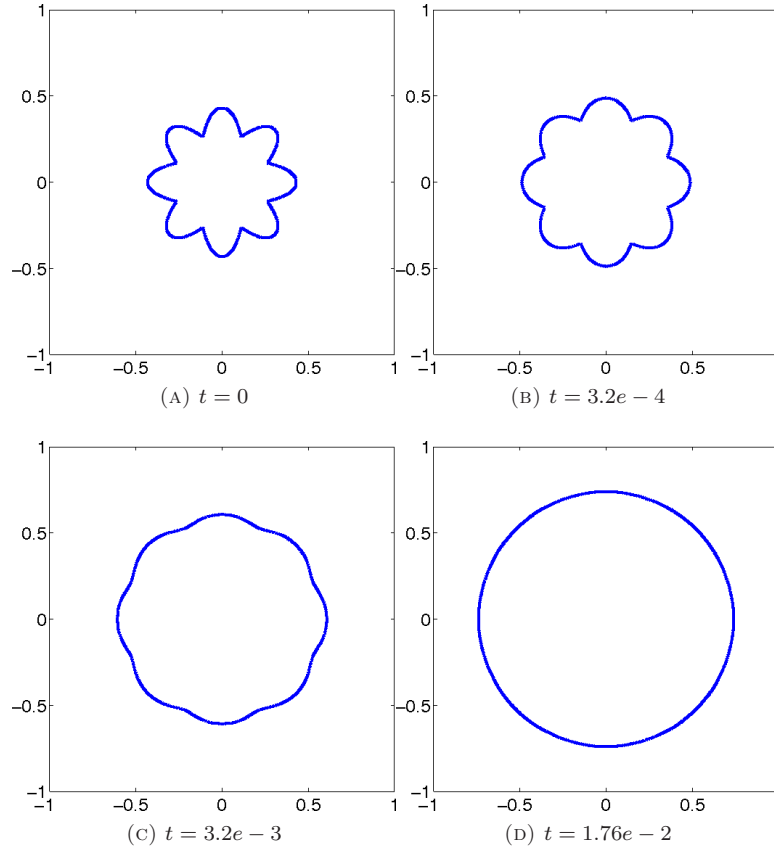


FIGURE 6. Support set of the initial value problem in Figure 5.

MATHEMATICS DEPARTMENT, UCLA
E-mail address: caflisch@math.ucla.edu

MATHEMATICS DEPARTMENT, UCLA
E-mail address: sjo@math.ucla.edu

MATHEMATICS DEPARTMENT, UCI
E-mail address: hschaeffer@ucla.edu

MATHEMATICS DEPARTMENT, UCLA
E-mail address: giangtran@math.ucla.edu

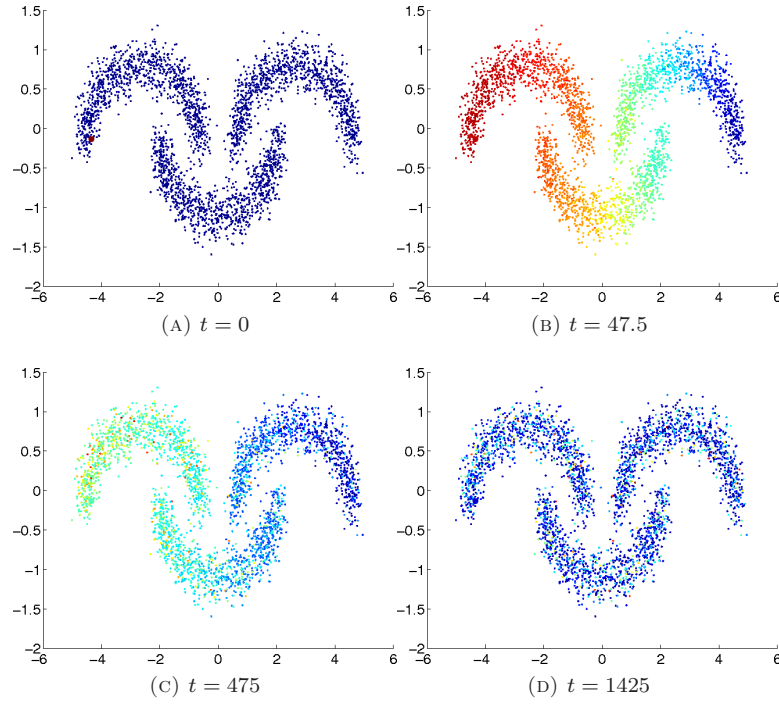


FIGURE 7. Solution of the initial value problem diffusing standard normalized graph Laplacian.

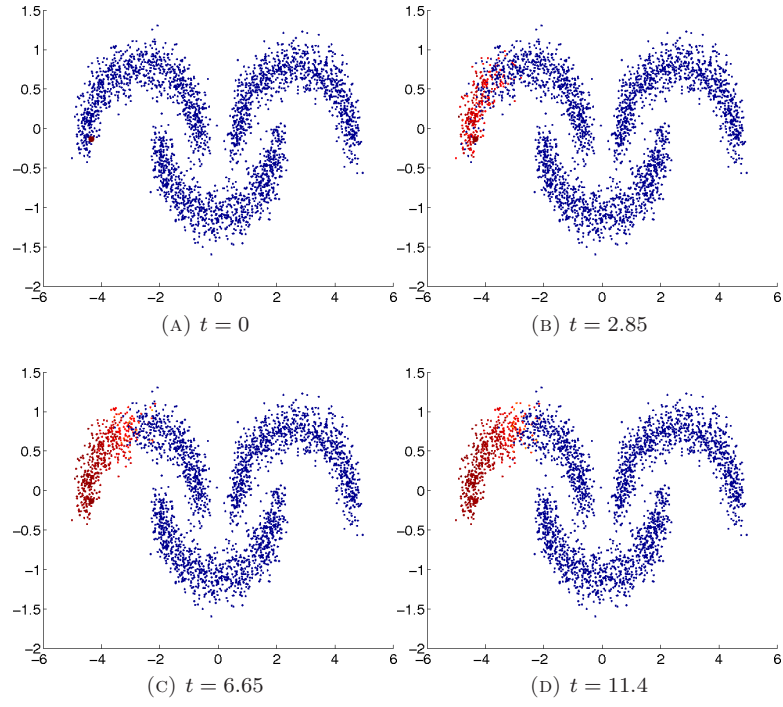


FIGURE 8. Solution of the initial value problem with the subgradient term, $\mu = 0.5e - 4$.